from fragments and reading inverted text (*4, 5, 12–15*). Nevertheless, KD patients are as unsuccessful as PD patients in establishing permanent records of recently occurring episodic events.

The obvious failures in episodic memory that are readily apparent in Korsakoff's disease, in contrast to similar impairments in PD patients, seem to result from disruptions in different cognitive mechanisms, and these in turn may both be unlike other syndrome-related cognitive failures. For example, the learning-memory failures in depressed patients can resemble those of PD patients, but unlike PD patients they can effectively organize events in memory, and are most likely to demonstrate cognitive dysfunctions on tasks that require sustained activity and effort but not on tasks that can be performed relatively automatically (*21*). For depressed patients and for learning-impaired children, cognitive dysfunction may be linked to levels of motivation, arousal, and activation, which is not the case in PD patients. It is also possible that some forms of memory impairment may result from a disruption in the functional and anatomical linkage between the reward-reinforcement and memory systems of the brain (*21, 28*). The memory pathology of KD patients may be of this type. A preliminary analysis and synthesis of findings based on the relationships between neurochemical, neuroanatomical, clinical, and cognitive findings supports this hypothesis.

A number of drugs can disrupt information processing in unimpaired subjects, and mimic some of these different forms of impairments in memory and learning. For example, alcohol produces a Korsakoff-like memory impairment in unimpaired subjects (*4*). In contrast, cholinergic antagonists produce a dementia-like learning-memory impairment associated with a disruption in access to information in semantic memory (*29*), while cholinergic agonists have some, albeit small, facilitating effect on memory in some senile dementia patients (*30, 31*). Catecholamine antagonists also produce distinctive cognitive changes that resemble those seen in clinical depression, while catecholaminergic agonists, such as amphetamine, enhance similar component cognitive processes (*32, 33*). Neuropeptides when administered to impaired or unimpaired subjects also produce a distinctive pattern of changes in information processing (*34*).

These different findings all suggest that human learning and memory are determined by multiple and discrete psychobiological mechanisms. A disruption of any one of these component processes can result in superficially similar but nevertheless fundamentally different cognitive changes. "Amnesias" can be seen as a final common pathway for a variety of cognitive dysfunctions. The development of effective therapeutic strategies for treating common learning-memory impairments requires that we begin to appreciate and define some of these forms and mechanisms of cognitive dysfunctions.

HERBERT WEINGARTNER
National Institute of Mental Health, Bethesda, Maryland 20205
JORDAN GRAFMAN
Walter Reed Army Medical Center, Washington, D.C. 20307
WILLIAM BOUTELLE
Veterans Administration Hospital, Northampton, Massachusetts 01060
WALTER KAYE
National Institute of Mental Health
PETER R. MARTIN
National Institute on Alcohol Abuse and Alcoholism, Bethesda, Maryland 20205

References and Notes

1. E. K. Warrington and L. Weiskrantz, in *The Physiological Basis of Memory*, A. Deutch, Ed. (Academic Press, New York (1973).
2. A. D. Baddeley and E. K. Warrington, *J. Verb. Learn. Verb. Behav.* **9**, 176 (1970).
3. L. S. Cermak, *Human Memory: Research and Theory* (Ronald, New York, 1972).
4. N. Butters and L. S. Cermak, *Alcoholic Korsakoff's Syndrome* (Academic Press, New York 1980).
5. E. K. Warrington, *Nature (London)* **228**, 628 (1970).
6. F. A. Huppert and M. Piercy, *Cortex* **12**, 8 (1976).
7. M. Moscovitch, in *Memory and Amnesia*, L. S. Cermak, Ed. (Erlbaum, Hillsdale, N.J., 1981).
8. L. L. Jacoby and D. Witherspoon, *Can. J. Psychol.*, in press.
9. L. L. Jacoby, in *Memory and Amnesia*, L. S. Cermak, Ed. (Erlbaum, Hillsdale, N.J., 1981).
10. E. Tulving and W. Donaldson, Eds., *Organization of Memory* (Academic Press, New York, 1972).
11. R. C. Atkinson, D. J. Hermann, K. T. Wescoust, *Theories of Cognitive Psychology*, R. L. Solso, Ed. (Erlbaum, Hillsdale, N.J., 1974).
12. S. Corkin, *Neuropsychologia* **6**, 255 (1968).
13. B. Milner, S. Corkin, H. L. Teuber, *ibid.*, p. 215.
14. N. J. Cohen and L. R. Squire, *Science* **210**, 207 (1980).
15. M. Kinsbourne and F. Wood, *Short-term Memory*, D. Deutsch and A. J. Deutsch Eds. (Academic Press, New York, 1975).
16. E. K. Warrington, *Neuropsychologia* **9**, 67 (1971).
17. R. S. Wilson, G. Rosenbaum, G. Brown, *J. Clin. Neuropsychol.* **1**, 49 (1979).
18. H. Bushke, *J. Verb. Learn. Verb. Behav.* **12**, 543 (1973).
19. H. Weingartner, E. D. Caine, M. H. Ebert, *J. Abnorm. Psychol.* **88**, 52 (1979).
20. H. Weingartner, W. Kaye, S. A. Smallberg, M. H. Ebert, J. C. Gillin, N. Sitaram, *ibid.* **90**, 187 (1981).
21. H. Weingartner, R. M. Cohen, J. Martello, D. L. Murphy, *Arch. Gen. Psychiatry* **38**, 42 (1981).
22. G. M. Kleiman, *Mem. Cognit.* **8**, 336 (1980).
23. G. Nottenburg and E. J. Shoben, *J. Exp. Soc. Psychol.* **16**, 329 (1980).
24. G. H. Bower, J. B. Black, T. J. Turner, *Cognit. Psychol.* **11**, 177 (1979).
25. J. de Ajuriaguerra and R. Tissot, in *Foundations of Language Development*, E. H. Lenneberg and E. Lenneberg, Eds. (Academic Press, New York, 1975), vols. 1 and 2.
26. N. J. Cohen and L. R. Squire, *Neuropsychologia*, **19**, 337 (1981).
27. F. A. Huppert and M. Percy, *Cortex* **15**, 385 (1979).
28. C. Kornetsky and R. V. Esposito, *Brain Res.* **209**, 496 (1981).
29. E. D. Caine, H. Weingartner, C. L. Ludlow, E. A. Cudahy, S. Wehry, *Psychopharmacology* **74**, 74 (1981).
30. K. L. Davis and R. C. Mohs, *New Engl. J. Med.* **301**, 946 (1975).
31. W. Kaye, N. Sitaram, H. Weingartner, J. C. Gillin, *Biol. Psychiatry* **17**, 275 (1982).
32. V. I. Reus, S. D. Targum, H. Weingartner, R. M. Post, *ibid.* **14**, (1979).
33. H. Weingartner *et al.*, *J. Abnorm. Psychol.* **89**, 25 (1980).
34. H. Weingartner *et al.*, *Science* **211**, 601 (1981).

30 August 1982

Spectral Consequences of Photoreceptor Sampling in the Rhesus Retina

Abstract. *Optical transforms were used to compute the power spectra of rhesus cones treated as arrays of image sampling points. Spectra were obtained for the central fovea, parafovea, periphery, and far periphery. All were consistent with a novel spatial sampling principle that introduces minimal noise for spatial frequencies below the Nyquist limits implied by local receptor densities, while frequencies above the nominal Nyquist limits are not converted into conspicuous moiré patterns, but instead are scattered into broadband noise. This sampling scheme allows the visual system to escape aliasing distortion despite a large mismatch between retinal image bandwidth and the Nyquist limits implied by extrafoveal cone densities.*

Like television and photography, vertebrate vision is based on discrete sampling of spatially continuous optical images. Spatial sampling of this sort can introduce two types of distortion: aliasing and noise (*1*). Aliasing is a moiré effect created by spatially regular sampling arrays, such as television rasters. Regular arrays allow perfect reconstruction of images whose spatial bandwidth does not exceed their Nyquist limit (half the sampling rate), but spatial frequencies above that limit are converted on a one-to-one basis into spurious low frequencies in the postsampling image. Noise is the analogous defect of spatially irregular sampling arrays, such as silver halide grains in photographic film. Perfectly random (Poisson) arrays have no Nyquist limit and produce no aliasing. The cost is a spectral scattering that affects high and low spatial frequencies

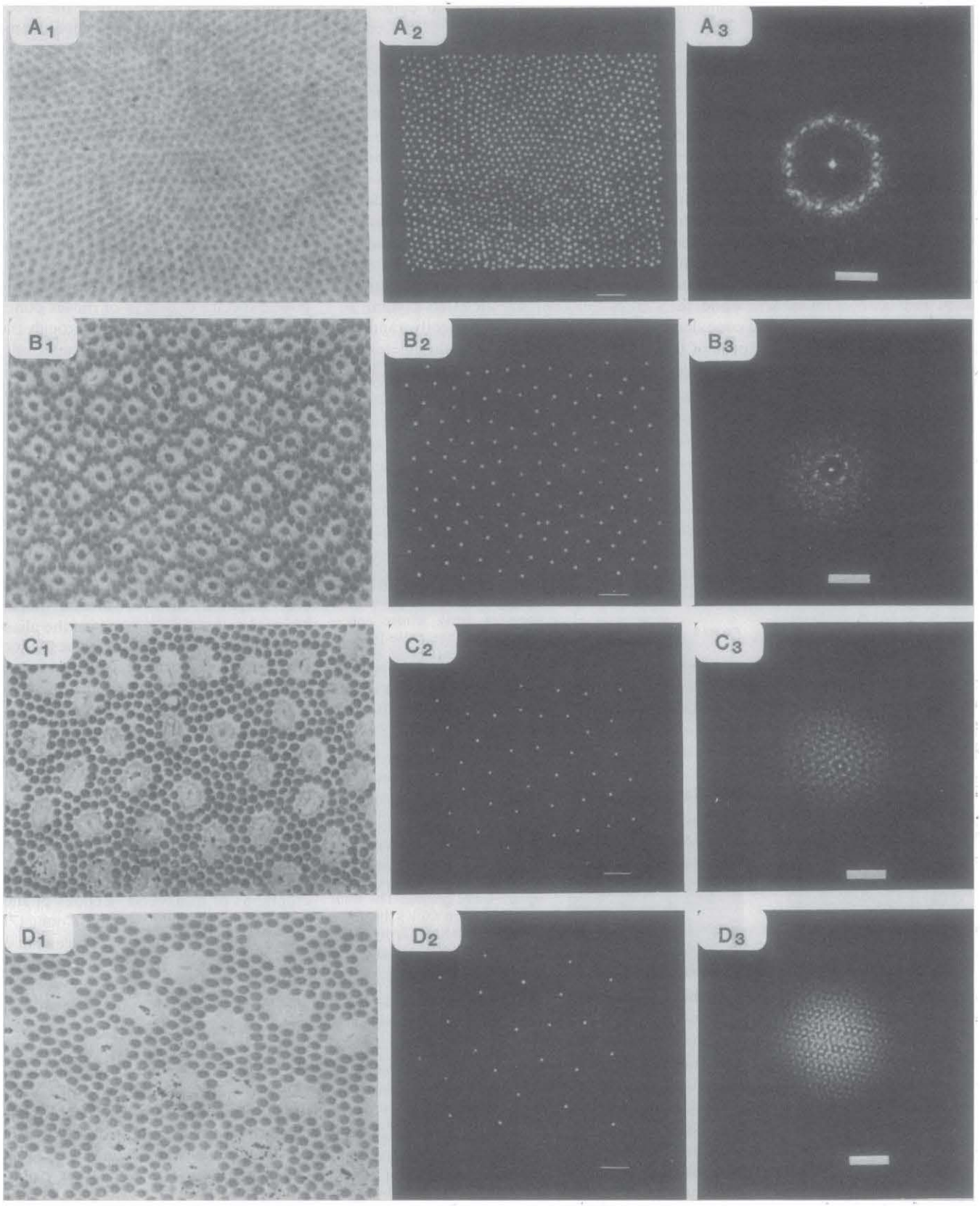

Fig. 1. (Column 1) Photomicrographs (×830) of 3.75 by 4.5 μm sections of rhesus retina (*7*). The sections subtended a visual angle of 15′ by 18′. (Column 2) Pinhole sampling arrays constructed from the cones in column 1. (Column 3) Power spectra (optical transforms) of column 2. Bars represent 120 cycle/deg. (A_1) Cone outer segments in the central fovea. (A_2) Sampling array, 1121 points; bar, 2′ on the retina. (B_1) Cone outer segments in the parafovea (eccentricity, approximately 6°). Cone tips are surrounded by empty space created by their inner segments. Each cone is circled by a ring of rods. (B_2) Sampling array, 123 points; bar, 2′. (C_1) Cone outer segments in the periphery (eccentricity, approximately 35°). The section passed near the tips of the cones, which are centered in the empty space created by their inner segments. Each cone is surrounded by two or three rows of rods. (C_2) Sampling array, 40 points; bar, 2.5′. (D_1) Cone outer segments from the far periphery (near the ora serrata). (D_2) Sampling array, 23 points; bar, 2.5′.

alike, however, so that the postsampling image is always masked by a veil of white noise.

The sampling elements of vertebrate daylight vision are the outer segments of the cone photoreceptors. In the rhesus monkey, and also in humans, this image sampling array has a puzzling feature: everywhere except the central fovea the Nyquist limits implied by local cone densities fall well below the spatial bandwidth of the retinal image. For example at 6° eccentricity the spatial bandwidth of the retinal image is 60 cycle/deg, just as in the central fovea (*2*), while the Nyquist limit implied by local cone density has fallen from its foveal peak of 60 cycle/deg (17,500 cones per square degree) to 15 cycle/deg (1200 cones per square degree) (*3*). Thus, if the cones formed spatially regular arrays one would expect extrafoveal photopic vision to be plagued by aliasing distortion. This does not occur—fine gratings viewed extrafoveally never look like coarse ones. What prevents this distortion?

An obvious possibility is spatial disorder in the receptor array. In both humans and rhesus monkeys the spatial arrangement of the cones is not perfectly regular, as can be seen from photomicrographs of cone mosaics (left column of Fig. 1). Neither is it perfectly random: receptor arrays fail a statistical test of nearest-neighbor distance against a Poisson null hypothesis (*4*). Thus, the spectral consequences of photoreceptor sampling cannot be immediately understood by analogy to either television or film. They can be determined analytically, however, if the Fourier spectrum of the receptor array is known, because the postsampling power spectrum of any image is the convolution of its original power spectrum with that of the sampling array (*5, 6*).

To determine the image sampling consequences of spatial disorder in the photoreceptor mosaic, I have computed the power spectra of arrays of rhesus cones treated as sampling points, through the use of optical transforms. The results (Fig. 1) indicate that throughout the retina the cones provide a novel form of optimal spatial sampling: optimal in the sense that minimal noise is introduced for spatial frequencies below the nominal Nyquist limits implied by local receptor densities (the limits that would obtain if the cones formed a regular lattice), while spatial frequencies above the local Nyquist limits are not aliased back into conspicuous moiré patterns but instead are scattered into broadband noise. Thus, the visual system avoids the aliasing distortion of high frequencies inherent in any regular arrangement of image sampling elements and simultaneously minimizes sampling noise for low frequencies that fall within its potential Nyquist bandwidths. These advantages stem from a quasi-random (that is, random but not Poisson) spatial sampling scheme that apparently has not been used in man-made image-recording devices.

The analysis was based on photomicrographs of transverse sections of rhesus retina prepared by R. W. Young (*7*). These showed the spatial arrangement of cone outer segments in 15′ by 18′ patches from the central fovea (Fig. $1A_1$), parafovea (Fig. $1B_1$), periphery (Fig. $1C_1$), and far periphery (Fig. $1D_1$). Each picture was converted to a sampling array by punching pinholes through black paper to mark the positions of the cones (middle column of Fig. 1). These pinhole arrays were photographed on a light table alongside strips of square-wave grating (which provided a reference pattern having a known spatial frequency on the scale of the retina), and photographically reduced to small (5 by 5 mm) high-contrast (Kodalith) transparencies. The power spectrum of each cone array was then computed in the form of an optical transform according to standard techniques (*8*). Light from a 2-mW He-Ne laser (Spectra Physics model 145) was

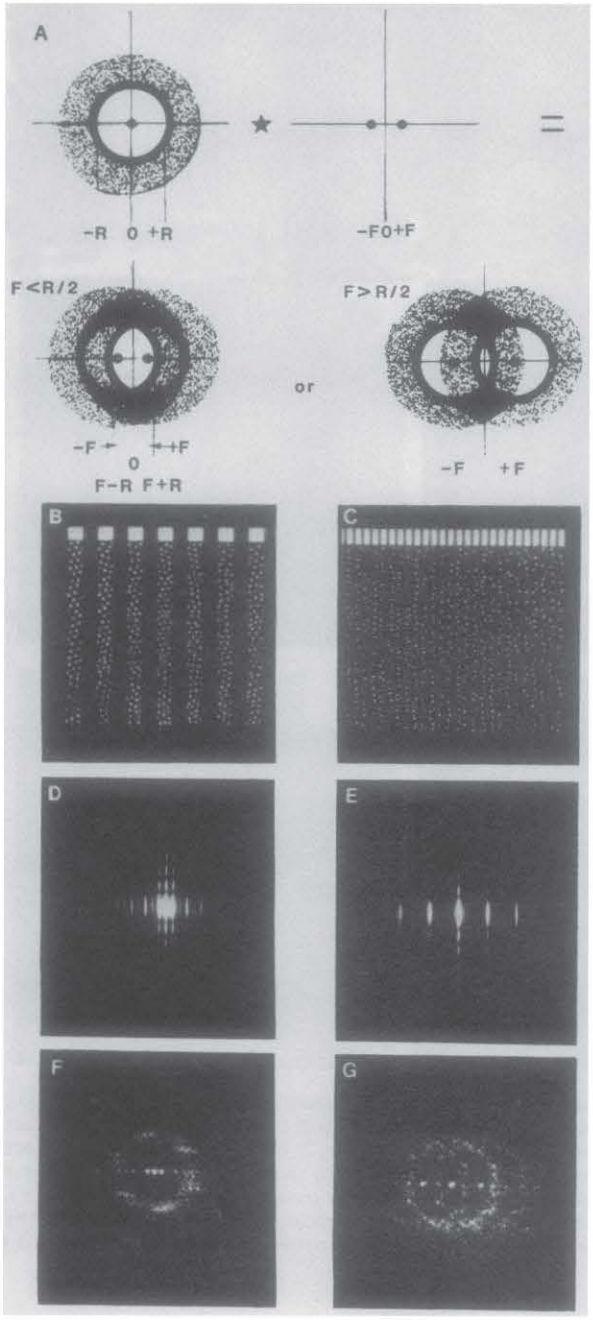

Fig. 2. (A) Spectral consequences of sampling an F cycle/deg spatial sinusoid with a sampling array whose spectrum follows the noise-free island pattern exhibited by the rhesus cones in Fig. 1. Island radius, R. Convolution of the array spectrum (top left) with the spectrum of a sinusoid (top right) yields deltas at $+F$ and $-F$ uncontaminated by noise when $F < R/2$ (bottom left). For $F > R/2$ the postsampling spectrum of the sinusoid contains broad bands of scattered low-frequency noise. (B) Foveal cone array (from Fig. $1A_2$) sampling a 24 cycle/deg square-wave grating. The thin strip at the top shows the grating alone. (C) Same array sampling an 86 cycle/deg grating. If these cones formed a regular lattice, their Nyquist frequency would be 53 cycle/deg, and an 86 cycle grating would alias back to 20 cycle/deg. [That is, it would look like the sampled grating in (B)]. Here there is no sign of such aliasing. (D) Power spectrum (optical transform) of the 24 cycle/deg strip in (B). (E) Power spectrum of the 86 cycle/deg strip in (C). (F) Power spectrum of 24 cycle/deg after sampling by foveal cones [that is, optical transform of the bottom part of (B)]. (G) Power spectrum of 86 cycle/deg after sampling by foveal cones.

diverged, collimated, passed through a transparency, and the resulting diffraction pattern (optical transform) was imaged on the far side by a plus lens. An enlarged image of the transform was cast on a distant rear projection screen by a final lens and photographed there with Polaroid P/N 55 film. Transforms of the grating strips (Fig. 2, D and E) were prepared simultaneously to provide a reference scale in spatial frequency space. The power spectra of the cones are shown in the right column of Fig. 1. Figure $1A_3$ shows the spectrum of the central fovea, which consists of a delta function at the origin surrounded by a circular island of empty space whose radius is on the order of 110 cycle/deg (*9*). Figure 2 illustrates the spectral consequencies of sampling with an array having a spectrum of this general form. Spatial frequencies less than half the radius of the noise-free island escape masking by noise, whereas higher frequencies are scattered into broadband noise containing energy at all spatial orientations (*10*). For an array of cones whose Nyquist frequency would be N cycle/deg if arranged in a spatial lattice (such as square or hexagonal; N would be essentially the same for both) the optimal radius for a noise-free island would be $2N$ cycle/deg. Young's cell count for the rhesus foveola is 19.4 cones per 100 μm^2 (*7*), which implies a nominal Nyquist frequency of 53 cycle/deg or a noise-free island radius of 106 cycle/deg. The spectra of the parafovea (Fig. $1B_3$) and periphery (Fig. $1C_3$) follow the same circular noise-free island pattern as the fovea, and there is a similar agreement between the radius of the islands (approximately 30 cycle/deg for the parafovea and 18 cycle/deg for the periphery); the optimal $2N$ values implied by the nominal Nyquist limits for these regions (28 cycle/deg for the parafovea, based on a cell count of 1.4 cones per 100 μm^2; and 19 cycle/deg for the periphery, based on a cell count of 0.6 cones per 100 μm^2). The spectrum of the far periphery (Fig. $1D_3$) also suggests the same pattern, but here the resolution limits of the apparatus (approximately 5 cycle/deg) would obscure a noise-free island at the optimal radius of 7 cycle/deg (0.3 cones per 100 μm^2).

Computer simulation combined with optical transform analysis shows that desert island spectra like those of the cones are characteristic of "Poisson disk" arrays—points scattered in the plane according to a Poisson distribution, but subject to the restriction of a fixed minimum distance between each point and its nearest neighbor (*11*). It seems possible that sampling arrays constructed on this basis might be useful in artificial image recording systems.

JOHN I. YELLOTT, JR.
Cognitive Science Group,
School of Social Sciences,
University of California, Irvine 92717

References and Notes

1. J. C. Dainty and R. Shaw, *Image Science* (Academic Press, London, 1974); D. E. Pearson, *Transmission and Display of Pictorial Information* Wiley, New York, 1975).
2. F. W. Campbell and R. W. Gubisch, *J. Physiol. (London)* **197**, 558 (1966); R. W. Gubisch, *J. Opt. Soc. Am.* **57**, 407 (1967); J. A. M. Jennings and W. N. Charman, *Vision Res.* **21**, 445 (1981).
3. G. Osterberg, *Acta Ophthalmol. Suppl.* **6**, 11 (1935); S. L. Polyak, *The Vertebrate Visual System* (Univ. of Chicago Press, Chicago, 1957); J. Yellott, B. Wandell, T. Cornsweet, in *Handbook of Physiology*, section 1, vol. 3, *Sensory Processes*, I. Darian-Smith, Ed. (American Physiological Society, Bethesda, Md., in press).
4. H. Wässle and H. T. Rieman, *Proc. R. Soc. London Ser. B* **200**, 441 (1978).
5. J. W. Goodman, *Introduction to Fourier Optics* (McGraw-Hill, New York, 1968); D. Nagel, *J. Opt. Soc. Am.*, in press.
6. P. F. Scott, *Distribution and Estimation of the Autocorrelation Function of a Randomly Sampled Signal* (Report No. 76 CRD 180, General Electric, Schenectady, N.Y., 1976).
7. R. W. Young, *J. Cell Biol.* **49**, 303 (1971), figures 10, 12, 14, and 16.
8. G. Harburn, C. A. Taylor, T. R. Welberry, *Atlas of Optical Transforms* (Cornell Univ. Press, Ithaca, 1975).
9. The same spectrum is also found in the human fovea [J. Yellott, *Vision Res.* **22**, 1205 (1982)]. No comparable analysis of extrafoveal human retina has yet been made. In general, however, human and rhesus eyes seem to be alike in all respects, and one would expect human results to be the same as those reported here for rhesus.
10. D. R. Williams and R. Collier [*Science* **221**, 385 (1983)] have shown that this scattered noise can mediate forced choice psychophysical discriminations between uniform fields and gratings at spatial frequencies much higher than the nominal Nyquist limits implied by receptor density.
11. J. I. Yellott, Jr., *Invest. Ophthalmol. Visual Sci.* **24** (Suppl. 3), 147 (Abstr.) (1983).
12. I thank P. Channing, T. Batey, M. Rudd, and J. W. Yellott for technical help; A. Ahumada, D. Nagel, and D. Williams for valuable discussions; and R. W. Young for permission to reproduce the photomicrographs in Fig. 1. Supported by a faculty research fellowship from the University of California, Sloan Foundation grant 80-6-12 to the UCI Cognitive Science Group, and National Aeronautics and Space Administration grant NCA2-OR345-301.

14 March 1983

Consequences of Spatial Sampling by a Human Photoreceptor Mosaic

Abstract. *The short wavelength color mechanism in the human visual system can distinguish gratings from uniform fields of the same average radiance at spatial frequencies that are twice as high as the highest at which it can resolve bars in the grating. This discrimination above the resolution limit is associated with a splotchy or mottled appearance of the grating similar to two-dimensional noise. The most plausible explanation for the mottled pattern is that it is a moiré pattern produced by aliasing (spatial undersampling) by an irregular and sparse mosaic of short wavelength cones.*

The design of imaging systems that discretely sample a continuous waveform is constrained by the problem of aliasing; if the sampling points are not close enough, high frequencies can masquerade in the reconstructed waveform as low frequencies (*1*). This constraint also applies to biological imaging systems: the mosaic of photoreceptors samples the retinal image. Indeed, there is behavioral evidence for aliasing by the regular ommatidial arrays in insect compound eyes (*2*). We now report evidence for aliasing in the human visual system when high-frequency gratings are seen via the mosaic of short wavelength [blue-sensitive (B)] cones.

Observers viewed a 10° violet grating superimposed on a 580-nm, 13.3° background intended to isolate the B mechanism (*3*). The axial chromatic aberration of the eye was compensated for by adjusting the optical distance of the violet grating relative to the fixated yellow background. Gratings were presented for 500 msec every third second. Between presentations, the grating was replaced by a uniform violet field that was coextensive with the grating and had the same average radiance. For each in a series of grating radiances, observers made two kinds of settings: they adjusted the grating spatial frequency until they could just detect the presence of bars in the target, and until they could just discriminate the grating from the uniform field that replaced it.

Consistent with the best earlier measures of B mechanism resolution (*4*), the acuity of two observers rose to about 10 and 14 cycle/deg (Fig. 1, A and B). At the highest radiance, one observer could distinguish between the grating and the uniform field at a spatial frequency of 23 cycle/deg and the other at 35 cycle/deg, more than twice the highest frequencies at which they could resolve bars. Similarly, a third, naïve observer (not shown) could resolve bars up to 11 cycle/deg yet could distinguish gratings from uniform fields up to 25 cycle/deg (*5*). As spatial frequency was increased at high grating